

## Development of UV-cured Plastic Scintillators Containing Water for Radioactivity Measurements of Seawater

Naru Hayashi<sup>1</sup> and Masanori Koshimizu<sup>1,2\*</sup>

<sup>1</sup>Department of Electronics and Materials Science, Shizuoka University,  
3-5-1 Johoku, Chuo-ku, Hamamatsu 432-8011, Japan

<sup>2</sup>Research Institute of Electronics, Shizuoka University,  
3-5-1 Johoku, Chuo-ku, Hamamatsu 432-8011, Japan

(Received October 30, 2025; accepted December 15, 2025)

**Keywords:** plastic scintillator, UV curing, aqueous solution, water-miscible monomer

UV-cured plastic scintillators capable of miscibility with aqueous solutions were developed and characterized. We selected a water-miscible monomer, M-240. The photoinitiator concentration and UV irradiation time were optimized to obtain samples having high scintillation light yields. All fabricated scintillators had an emission peak at approximately 450 nm and an excitation peak at 350–400 nm in the photoluminescence emission and excitation spectra, respectively. The scintillation spectra also had a peak at around 450 nm, which is attributed to the emission of 1,4-bis(5-phenyl-2-oxazolyl)benzene included in the scintillators as wavelength-shifting molecules. Using the optimized conditions, we evaluated the effect of adding distilled water on the appearance of the scintillators and their scintillation light yields at different concentrations of the fluorescent molecules. The addition of distilled water up to approximately 8 wt% resulted in a decrease in the scintillation light yield by less than 40%. On the basis of these results, we have successfully developed UV-cured plastic scintillators containing aqueous solutions.

### 1. Introduction

Scintillators are materials that convert the energy of ionizing radiation to luminescence. Coupled with photodetectors such as photomultiplier tubes (PMTs), they enable the detection of ionizing radiation as electric signals. Scintillators are broadly classified into inorganic and organic types. Inorganic scintillators include single crystals and glasses.<sup>(1–11)</sup> Because they contain high-Z elements, they efficiently absorb  $\gamma$ -rays and X-rays, and have high scintillation light yields. Organic scintillators include crystals, liquids, and plastics.<sup>(12–17)</sup> They are characterized by fast decay times and low material costs compared with inorganic scintillators.

Liquid scintillators are widely used for radioactivity measurements across particle physics,<sup>(18)</sup> environmental monitoring,<sup>(19)</sup> and analyses of elemental behavior in biological systems.<sup>(20)</sup> In investigations of element dynamics *in vivo*, liquid scintillation counting (LSC) is commonly

\*Corresponding author: e-mail: [koshimizu.masanori@shizuoka.ac.jp](mailto:koshimizu.masanori@shizuoka.ac.jp)  
<https://doi.org/10.18494/SAM6036>

employed for studies of elemental kinetics *in vivo*.<sup>(21)</sup> Applications include RNA analysis,<sup>(22)</sup> detection of organically bound tritium excreted by organisms,<sup>(23)</sup> tracking DNA adducts,<sup>(24)</sup> and isomer-specific regulation in human preadipocytes.<sup>(25)</sup> In particle-physics detectors, liquid scintillators are used primarily for neutrino measurements: Borexino employs 278 tons of liquid scintillator,<sup>(18)</sup> and the Kamioka Liquid Scintillator Antineutrino Detector likewise performs neutrino observations using a liquid scintillator.<sup>(26)</sup> In environmental fields, LSC is also used for tritium monitoring by detecting the beta particles emitted from  $^3\text{H}$  and the identification of radionuclides in food and drinking water.<sup>(27-29)</sup> Surveys of radionuclides in seawater typically rely on LSC, in which a concentrated sample is mixed with a scintillation cocktail and counted.<sup>(30,31)</sup> However, it has the disadvantage that liquid samples using LSC are less convenient than solid samples. Additionally, the concentration process is complex. Moreover, the organic solvents used in liquid scintillators pose risks to human health.<sup>(32,33)</sup>

To address these difficulties, we considered applying plastic scintillators to the detection of radionuclides in aqueous solution. Plastic scintillators offer low material cost: for example, in high-energy physics detectors, CsI crystals were replaced with plastic scintillators to reduce cost.<sup>(34)</sup> If scintillators can be fabricated from ultraviolet (UV)-curable resins, arbitrary shapes can be produced readily in a manner analogous to 3D printing.<sup>(35)</sup> The scintillation light yields of UV-cured plastic scintillators in previous studies have generally been lower than those of commercial plastic scintillators. Although the scintillation light yields of conventional plastic scintillators were about 10000 photons/MeV,<sup>(36)</sup> those of UV-cured plastic scintillators were less than 8000 photons/MeV.<sup>(37)</sup> By optimizing the composition and processing, we increased the scintillation light yield to 9600 photons/MeV.<sup>(38,39)</sup>

Plastic scintillators have been considered for radioactivity measurements. In conventional approaches, it is necessary to prepare the setup with the measurement aqueous solution samples positioned adjacent to the scintillators. For example, plastic-scintillator particles have been dispersed into the solutions, and then, the scintillation from the mixture was counted using the LSC system.<sup>(40)</sup> If UV-cured plastic scintillators replace the liquid scintillation cocktail, the sample handling would be simplified. In addition, unlike LSC, which typically requires a dedicated counter, the UV-cured plastic scintillator enables measurements using common radiation detection equipment. Furthermore, while LSC generally requires the preconcentration of aqueous samples, if plastic scintillators containing an aqueous solution can be fabricated, the radionuclide-containing aqueous solution can be mixed into the solid scintillators, enabling measurements without preconcentration.

In this study, we first investigated monomers that are miscible with distilled water. To impart moderate hydrophilicity, we selected candidate monomer compounds containing a ketone group and assessed miscibility by mixing with distilled water. For the selected monomer, we then optimized the concentrations of the photoinitiator and fluorescent molecules and measured the scintillation light yields of the samples prepared without distilled water. Finally, we fabricated distilled-water-loaded samples. In addition, we investigated the effects of the concentrations of the fluorescent molecules and distilled water on the scintillation light yields.

## 2. Experimental Methods

The preparation method of the plastic scintillators is modified from our previously reported procedure.<sup>(38,39)</sup> M-240 was supplied by Toagosei.<sup>(41)</sup> Irgacure TPO (diphenyl[2,4,6-trimethylbenzoyl]phosphine oxide, >98.0 %) and POPOP (1,4-bis[2-(5-phenyloxazolyl)]benzene, >98.0 %) were purchased from Tokyo Chemical Industry. DPO (2,5-diphenyloxazole, >99 %) was purchased from Sigma-Aldrich. All materials were used without further purification.

Figure 1 shows the structure of M-240. Because this monomer has a ketone group, we expect high miscibility with water. Indeed, we selected this molecule because it could be mixed with distilled water and subsequently cured. Irgacure TPO, as a photoinitiator, was added to M-240 at different concentrations. Subsequently, the fluorescent molecules DPO and POPOP were added. For some samples, we added distilled water. The molar ratio of DPO:POPOP was 80:1. The resin solutions were heated in an oil bath at 80 °C for 4–5 h to dissolve the fluorescent molecules and subsequently irradiated with UV light (AS ONE, LUV-16, 1820 μW/cm<sup>2</sup>) at 365 nm to solidify the scintillators. We optimized the concentrations of the photoinitiator and fluorescent molecules and the UV irradiation time to achieve a high scintillation light yield.

The emission and excitation spectra were measured using a fluorescent spectrophotometer (RF-5300PC, Shimadzu). The scintillation spectra were obtained under X-ray irradiation (XRB80N100, Spellman). The scintillation from the samples was detected with a CCD detector (Newton 920, Andor) equipped with a monochromator (Shamrock 163, Andor). The pulse height spectra of the scintillation detectors equipped with the samples were obtained for 0.0595 MeV gamma rays from <sup>241</sup>Am. The scintillation from the samples was detected using a PMT (R7600U-200, Hamamatsu Photonics) applied at 700 V. Signals were sent to a preamplifier (113 Preamplifier, ORTEC) and a main amplifier (572 Amplifier, ORTEC). The signals from the main amplifier were accumulated using a multichannel analyzer (MCA8000D, Amptek) into histograms as the pulse height spectra. The scintillation light yields were estimated on the basis of the peak channels of EJ-256 in the spectra.

## 3. Results and Discussion

Figure 2 shows the photographs of the samples containing Irgacure TPO at 0.17 wt%, DPO at 23 wt%, and POPOP at 0.47 wt% without distilled water. As seen in the photograph under room light, the sample was transparent without cracks. Under UV light, the sample emits blue fluorescence.

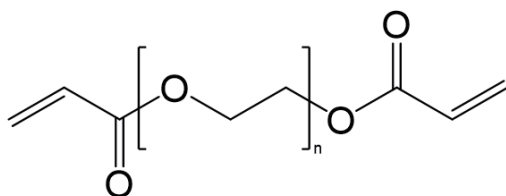


Fig. 1. Structure of M-240.

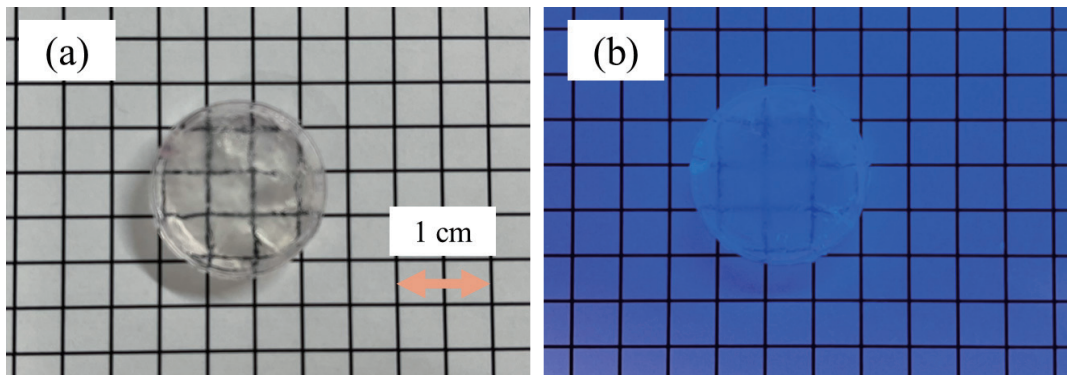


Fig. 2. (Color online) Photographs of scintillator sample containing Irgacure TPO at 0.17 wt%, DPO at 23 wt%, and POPOP at 0.47 wt% without distilled water (a) under room light and (b) under UV light at 365 nm.

Figure 3 shows the emission and excitation spectra of the sample containing Irgacure TPO at 0.17 wt%, DPO at 23 wt%, and POPOP at 0.47 wt%. This sample had the highest scintillation light yield among all samples. The emission spectra of all the samples were similar and had a peak at approximately 450 nm, which originates from POPOP added as the wavelength shifter. The excitation spectra had a broad peak at 350–385 nm, which is also attributed to POPOP. Figure 4 shows the scintillation spectrum of the same sample containing Irgacure TPO at 0.17 wt%, DPO at 23 wt%, and POPOP at 0.47 wt%. The spectrum had a peak with the maximum emission wavelength of 450 nm, which is attributed to the emission of POPOP used as the wavelength shifter. The scintillation spectra of all the samples were similar.

Figure 5 shows the pulse height spectra of the samples containing DPO and POPOP at concentrations of 16 and 0.34 wt%, respectively (DPO:POPOP = 80:1 in molar ratio), and Irgacure TPO at a concentration of 0.10, 0.17, or 0.27 wt% with respect to M-240, and EJ-256 as a reference. The peak channels of the samples containing Irgacure TPO at 0.27 wt% were the lowest, followed by samples with 0.10 wt% and 0.17 wt%. Table 1 shows the scintillation light yields of the samples with different Irgacure TPO concentrations. The scintillation light yields were estimated by comparing the peak channels to those of EJ-256 (5200 photons/MeV) as the reference. The pulse height spectra was fitted with sums of two Gaussian functions to estimate the peak channel. The scintillation light yields discussed hereafter were also estimated using the same procedure. The sample containing Irgacure TPO at 0.17 wt% exhibits the highest scintillation light yield. The dependence of the scintillation light yield on the concentration of the photoinitiator is consistent with the findings of our previous study,<sup>(37)</sup> where M-211B was used as the monomer. The scintillation light yields of the samples containing Irgacure TPO concentrations at either below or above 0.17 wt% were lower, possibly because the photoinitiator at low concentrations does not sufficiently initiate polymerization, whereas at high concentrations, quenching by the photoinitiator becomes severe. On the basis of these results, we prepared samples containing Irgacure TPO at 0.17 wt% hereafter.

Table 2 shows the compositions of the samples containing Irgacure TPO at a concentration of 0.17 wt% with respect to M-240, DPO and POPOP at different concentrations irradiated with UV light for 5 h, and EJ-256 as a reference. Figure 6 shows the pulse height spectra of the samples containing DPO and POPOP at different concentrations. The samples containing DPO

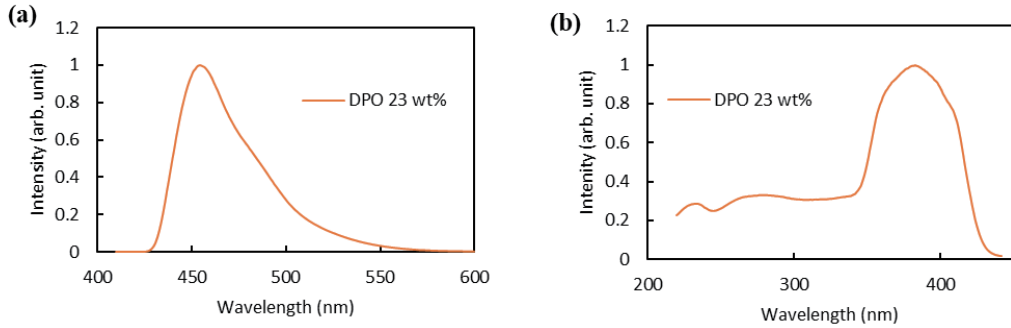


Fig. 3. (Color online) (a) Emission ( $\lambda_{ex} = 400$  nm) and (b) excitation spectra ( $\lambda_{em} = 450$  nm) of the sample containing Irgacure TPO at 0.17 wt%, DPO at 23 wt%, and POPOP at 0.47 wt%, which had the highest scintillation light yield among the samples.

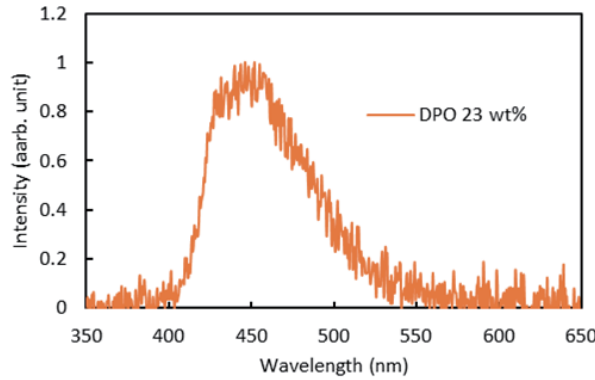


Fig. 4. (Color online) Scintillation spectrum of plastic scintillator sample containing Irgacure TPO at 0.17 wt%, DPO at 23 wt%, and POPOP at 0.47 wt%.

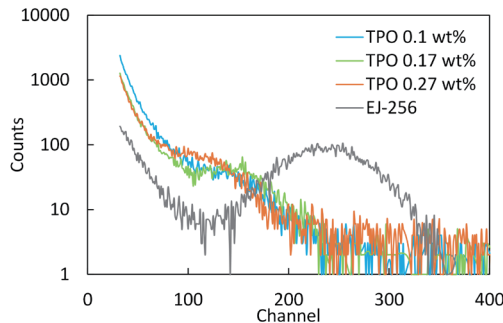


Fig. 5. (Color online) Pulse height spectra of samples containing DPO and POPOP at concentrations of 16 and 0.34 wt%, Irgacure TPO at concentrations of 0.1, 0.17, and 0.27 wt% with respect to M-240, and a commercially available plastic scintillator, EJ-256.

Table 1

Scintillation light yields of samples containing DPO and POPOP at concentrations of 16 and 0.34 wt%, respectively, and Irgacure TPO at concentrations of 0.1, 0.17, and 0.27 wt% with respect to M-240.

| Concentration of Irgacure TPO | Scintillation light yields (photons/MeV) |
|-------------------------------|--|
| 0.1 wt%                       | 2800                                     |
| 0.17 wt%                      | 3100                                     |
| 0.27 wt%                      | 2200                                     |

Table 2

Compositions and scintillation light yields of samples containing Irgacure TPO at a concentration of 0.17 wt% with respect to M-240, and DPO and POPOP at different concentrations, irradiated with UV light for 5 h.

| M-240 (wt%)                              | 91   | 86   | 83   | 76   |
|--|------|------|------|------|
| Irgacure TPO (wt%)                       | 0.15 | 0.15 | 0.14 | 0.13 |
| DPO (wt%)                                | 8.9  | 13   | 16   | 23   |
| POPOP (wt%)                              | 0.18 | 0.26 | 0.34 | 0.47 |
| Scintillation light yields (photons/MeV) | 2100 | 2300 | 2600 | 2600 |

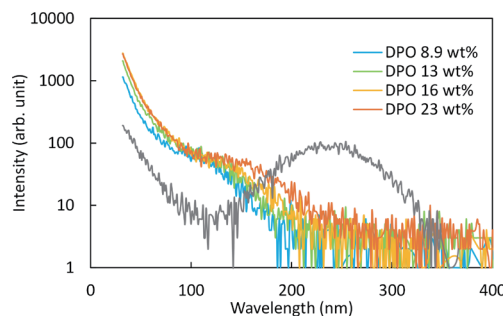


Fig. 6. (Color online) Pulse height spectra of samples containing Irgacure TPO at a concentration of 0.17 wt% with respect to M-240, and DPO and POPOP at different concentrations, irradiated with UV light for 5 h, and a commercially available plastic scintillator, EJ-256.

at higher than 28 wt% precipitated DPO during the UV curing. We could not prepare samples containing DPO at higher than 28 wt% owing to the precipitating DPO during the UV curing. As summarized in Table 2, the samples with the higher concentrations of DPO and POPOP had higher scintillation light yields. The scintillation light yield of the sample containing DPO at 23 wt% and POPOP at 0.47 wt% was 2600 photons/MeV, which was the highest among the samples. On the basis of these results, we then prepared samples containing DPO and POPOP at the concentrations of 23 and 0.47 wt%, respectively.

Figure 7 shows the pulse height spectra of the samples containing Irgacure TPO at a concentration of 0.17 wt% with respect to M-240, and DPO and POPOP at the concentrations of 23 and 0.47 wt%, respectively, synthesized at different UV irradiation times. Table 3 shows their scintillation light yields. The scintillation light yield of the sample irradiated with UV light for 3 h was the highest. The samples irradiated with UV light for longer than 24 h exhibited a yellow color owing to the coloration of DPO by the UV light, which was reported in Ref. 37. In contrast, the samples irradiated with UV light for less than 1 h were not cured sufficiently. The optimized UV irradiation time was 5 h in previous studies in which M-211B was used as the monomer.<sup>(37,38)</sup> In this study, the optimized UV irradiation time was 3 h because a different monomer was used. On the basis of these results, we prepared samples with UV light irradiation for 3 h.

We further investigated the effects of the addition of distilled water on the sample appearance and scintillation light yields. The samples containing distilled water and DPO and POPOP at the optimal concentrations had a thin white layer over the entire surface, while the inside of the samples was transparent. In addition, part of the top surface of the samples was not fully solidified. Because the samples containing only fluorescent molecules or distilled water were

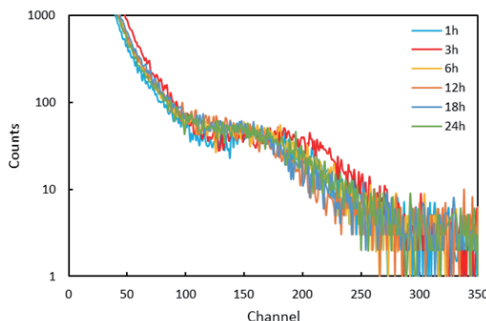


Fig. 7. (Color online) Pulse height spectra of samples containing Irgacure TPO at a concentration of 0.17 wt% with respect to M-240, and DPO and POPOP at concentrations of 23 and 0.47 wt%, respectively, synthesized with different UV irradiation times.

Table 3

Scintillation light yields of samples containing Irgacure TPO at a concentration of 0.17 wt% with respect to M-240, and DPO and POPOP at concentrations of 23 and 0.47 wt%, respectively, synthesized with different UV irradiation times.

| UV irradiation time | Scintillation light yields (photons/MeV) |
|---------------------|--|
| 1 h                 | 3400                                     |
| 3 h                 | 3700                                     |
| 6 h                 | 3200                                     |
| 12 h                | 2600                                     |
| 18 h                | 2900                                     |
| 24 h                | 2900                                     |

transparent and fully cured, this result indicates that both distilled water and the fluorescent molecules influence the curing characteristics and their appearance. The partially solidified samples containing distilled water were not cured completely even after an additional 3 h of UV irradiation. The fluorescent molecules and water molecules do not participate in the polymerization reaction and interfere with the formation of the polymer network, which results in the inhibition of the solidification reaction. Therefore, to obtain transparent and fully cured samples containing both distilled water and the fluorescent molecules, we varied the concentrations of both the fluorescent molecules and distilled water and investigated the appearance of the resulting samples along with their scintillation light yields. Table 4 shows the compositions and photographs of samples containing distilled water and fluorescent molecules, synthesized with UV light irradiation for 3 h. We observed that this change in appearance owing to incomplete curing depended on the concentrations of the fluorescent molecules and the distilled water. As the fluorescent molecule concentration increased, the surface irregularities of the samples owing to incomplete curing became more pronounced. Figure 8 shows the pulse height spectra of the samples containing Irgacure TPO at a concentration of 0.17 wt% with respect to M-240, synthesized with UV light irradiation for 3 h, containing (a) DPO at a concentration of 22 or 21 wt% and distilled water at 2.3, 3.7, or 7.1 wt%, (b) DPO at a concentration of 16 or 15 wt%, and distilled water at 2.4, 4.0, or 7.7 wt%, and (c) DPO at a concentration of 8.7, 8.5, or 8.2 wt% and distilled water at 2.7, 4.3, or 8.3 wt%. In Fig. 8(c), the spectra show no noticeable peaks, and the scintillation light yields could not be estimated. Table

Table 4

Compositions, photographs, and scintillation light yields of samples containing distilled water and fluorescent molecules at different concentrations, synthesized with UV light irradiation for 3 h.

| Composition (wt%) and scintillation light yield (photons/MeV) |      |      |      |      |      |
|---|------|------|------|------|------|
| M-240   | 88   |      | 87   |      | 83   |
| Irgacure TPO  | 0.15 |      | 0.14 |      | 0.14 |
| DPO   | 8.7  |      | 8.5  |      | 8.2  |
| POPOP   | 0.18 |      | 0.18 |      | 0.17 |
| Distilled water   | 2.7  |      | 4.3  |      | 8.3  |
| Scintillation light yield                                     |      | —    | —    | —    | —    |
| M-240   | 81   |      | 80   |      | 77   |
| Irgacure TPO  | 0.14 |      | 0.13 |      | 0.13 |
| DPO   | 16   |      | 16   |      | 15   |
| POPOP   | 0.33 |      | 0.32 |      | 0.31 |
| Distilled water   | 2.4  |      | 4.0  |      | 7.7  |
| Average scintillation light yield                             |      | 2800 | 2400 | 1700 |      |
| M-240   | 75   |      | 74   |      | 71   |
| Irgacure TPO  | 0.13 |      | 0.12 |      | 0.12 |
| DPO   | 22   |      | 22   |      | 21   |
| POPOP   | 0.46 |      | 0.45 |      | 0.43 |
| Distilled water   | 2.3  |      | 3.7  |      | 7.1  |
| Average scintillation light yield                             |      | 3600 | 3300 | 3200 |      |

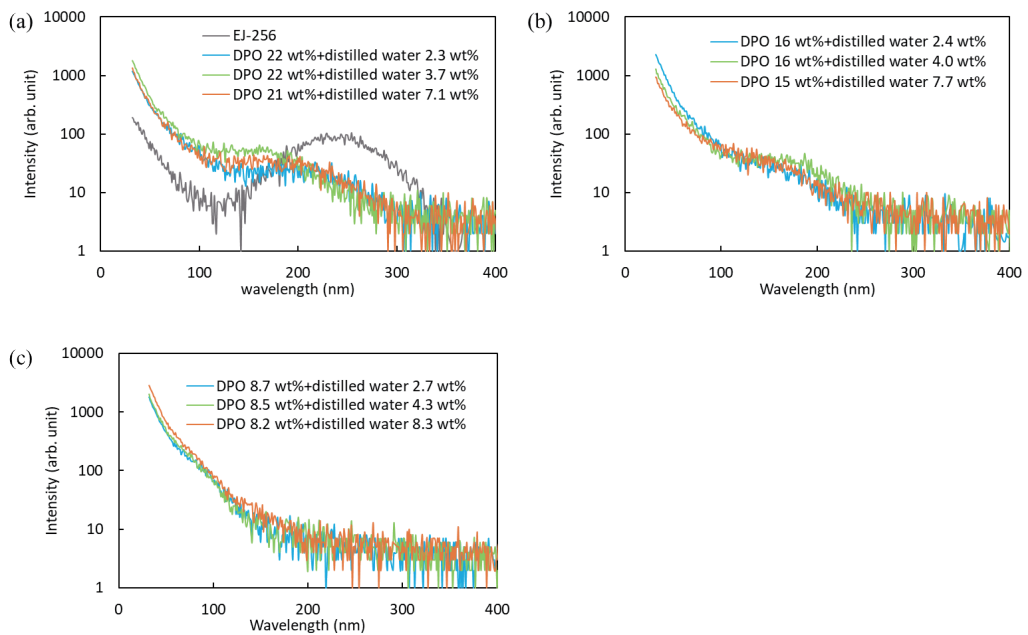


Fig. 8. (Color online) Pulse height spectra of samples containing Irgacure TPO at a concentration of 0.17 wt% with respect to M-240, synthesized with UV light irradiation for 3 h, containing (a) DPO at a concentration of 22 or 21 wt% and distilled water at 2.3, 3.7, or 7.1 wt%, (b) DPO at a concentration of 16 or 15 wt% and distilled water at 2.4, 4.0, or 7.7 wt%, and (c) DPO at a concentration of 8.7, 8.5, or 8.2 wt% and distilled water at 2.7, 4.3, or 8.3 wt%.

4 shows the scintillation light yields of these samples. Samples with the same compositions were fabricated and evaluated. As summarized in Table 4, with increasing fluorescent molecule concentration, the scintillation light yield increased, whereas increasing the distilled water concentration decreased the scintillation light yield. Compared with the sample without distilled water having a scintillation light yield of 3700 photons/MeV as presented in Table 3, the samples containing DPO at concentrations of 21 or 22 wt% showed scintillation light yields that were reduced by 0.0%, 14%, and 16% with the addition of distilled water at 2.3, 3.7, and 7.1 wt%, respectively. Also, compared with the sample without distilled water having a scintillation light yield of 2700 photons/MeV, the samples containing DPO at concentrations of 15 or 16 wt% showed scintillation light yields that were reduced by -3.7 %, 3.7 %, and 37 % following the addition of distilled water at 2.4, 4.0, and 7.7 wt%, respectively. A part of the radiation energy is consumed to ionize water and does not contribute to scintillation. Hence, the scintillation light yield decreased following the addition of water. It would be feasible to fully remove water from the liquid mixture containing aqueous solution of radioactive isotopes before curing, and the scintillation light yield is expected to increase after the removal of water and curing. In addition, whether radioactive isotopes remain is unclear because it depends on the type of isotope. If they remain as inorganic compounds, they will precipitate. The addition of distilled water up to approximately 8 wt% resulted in a decrease in the scintillation light yield by less than 40%. The minimum necessary water content is unclear because there are no previous studies on plastic scintillators containing water. A higher water content allows the inclusion of a larger number of radioactive isotopes. Nevertheless, in this work, we successfully added up to ~8 wt% water, which is regarded as one of the main constituents. From this viewpoint, the inclusion of water in the plastic scintillators in this study is successful.

#### 4. Conclusions

We developed UV-cured plastic scintillators containing aqueous solutions. We first investigated monomers miscible with water and optimized both the photoinitiator concentration and the UV irradiation time. All the scintillators have a peak in the photoluminescence emission and scintillation spectra at approximately 450 nm, which is attributed to POPOP. Using the optimized conditions, we investigated the effect of water addition on the scintillation light yield at different fluorescent molecule concentrations. The addition of distilled water up to approximately 8 wt% resulted in a decrease in the scintillation light yield by less than 40%. On the basis of these results, we have successfully developed UV-cured plastic scintillators containing aqueous solutions.

## Acknowledgments

This research was supported by a Grant-in-Aid for Scientific Research (A) (No. 22H00308: 2022–2025). Part of this study was supported by the Cooperative Research Project of the Research Center for Biomedical Engineering of the Ministry of Education, Culture, Sports, Science, and Technology and a Marine Informatics Research Program provided by Grants for the Revitalization of Regional Universities and Industries (Suruga Bay Marine DX Advanced Hub initiative).

## References

- 1 M. Koshimizu, K. Tanahashi, Y. Fujimoto, and K. Asai: *Sens. Mater.* **37** (2025) 539. <https://doi.org/10.18494/SAM5448>
- 2 T. Kunikata, K. Okazaki, H. Kimura, S. Takase, T. Kato, D. Nakauchi, N. Kawaguchi, and T. Yanagida: *Sens. Mater.* **37** (2025) 563. <https://doi.org/10.18494/SAM5428>
- 3 M. Ishida, A. Watanabe, H. Kawamoto, Y. Fujimoto, and K. Asai: *Sens. Mater.* **37** (2025) 607. <https://doi.org/10.18494/SAM5482>
- 4 Y. Endo, K. Ichiba, D. Nakauchi, T. Kato, N. Kawaguchi, and T. Yanagida: *Sens. Mater.* **36** (2024) 473. <https://doi.org/10.18494/SAM4758>
- 5 H. Fukushima, D. Nakauchi, T. Kato, N. Kawaguchi, and T. Yanagida: *Sens. Mater.* **36** (2024) 489. <https://doi.org/10.18494/SAM4762>
- 6 H. Kimura, H. Fukushima, K. Watanabe, T. Fujiwara, H. Kato, M. Tanaka, T. Kato, D. Nakauchi, N. Kawaguchi, and T. Yanagida: *Sens. Mater.* **36** (2024) 507. <https://doi.org/10.18494/SAM4767>
- 7 K. Miyazaki, D. Nakauchi, T. Kato, N. Kawaguchi, and T. Yanagida: *Sens. Mater.* **36** (2024) 515. <https://doi.org/10.18494/SAM4756>
- 8 K. Yamabayashi, K. Okazaki, D. Nakauchi, T. Kato, N. Kawaguchi, and T. Yanagida: *Sens. Mater.* **36** (2024) 523. <https://doi.org/10.18494/SAM4760>
- 9 K. Miyajima, A. Nishikawa, T. Kato, D. Nakauchi, N. Kawaguchi, and T. Yanagida: *Sens. Mater.* **37** (2025) 481. <https://doi.org/10.18494/SAM5436>
- 10 H. Fukushima, R. Tsubouchi, T. Matsuura, T. Yoneda, and T. Yanagida: *Sens. Mater.* **37** (2025) 487. <https://doi.org/10.18494/SAM5438>
- 11 S. Muneta, N. Kawano, D. Nakauchi, T. Kato, K. Okazaki, K. Ichiba, T. Kunikata, A. Nishikawa, K. Miyazaki, F. Kagaya, K. Shinozaki, and T. Yanagida: *Sens. Mater.* **37** (2025) 509. <https://doi.org/10.18494/SAM5441>
- 12 C. Kim, W. Lee, A. Melis, A. Elmughrabi, K. Lee, C. Park, and J. Yeom: *Crystals* **11** (2021) 669. <https://doi.org/10.3390/cryst11060669>
- 13 F. Maddalena, L. Tjahjana, A. Xie, Arramel, S. Zeng, H. Wang, P. Coque, W. Drozdowski, C. Dujardin, C. Dang, and M. D. Birowosuto: *Crystals* **9** (2019) 88. <https://doi.org/10.3390/cryst9020088>
- 14 I. Shimizu and M. Chen: *Front. Phys.* **7** (2019) 33. <https://doi.org/10.3389/fphy.2019.00033>
- 15 A. Watanabe, A. Sato, M. Koshimizu, K. Watanabe, Y. Fujimoto, and K. Asai: *Phys. Chem. Chem. Phys.* **26** (2024) 9329. <https://doi.org/10.1039/d4cp00042k>
- 16 H. Tsukahara, M. Koshimizu: *J. Mater. Sci.: Mater. Electron.* **36** (2025) 1223. <https://doi.org/10.1007/s10854-025-15288-8>
- 17 V. N. Salimgareeva, and S. V. Kolesov: *Instrum. Exp. Tech.*, **48** (2005) 273. <https://doi.org/10.1007/s10786-005-0052-8>
- 18 G. Bellini: *Annu. Rev. Nucl. Part. Sci.* **74** (2024) 369. <https://doi.org/10.1146/annurev-nucl-102622-021701>
- 19 P. H. Santschi, C. Xu, S. Zhang, K. A. Schwehr, P. Lin, C. M. Yeager, and D. I. Kaplan: *J. Environ. Radioact.* **171** (2017) 226. <https://doi.org/10.1016/j.jenvrad.2017.02.023>
- 20 P. L. Goff, M. Fromm, L. Vichot, P. M. Badot, and P. Guéitat: *Environ. Int.* **65** (2014) 116. <https://doi.org/10.1016/j.envint.2013.12.020>
- 21 X. Hou: *J. Radioanal. Nucl. Chem.* **318** (2018) 1597. <https://doi.org/10.1007/s10967-018-6258-6>
- 22 Z. Yang, G. Vilkaitis, B. Yu, S. Klimašauskas, and X. Chen: *Methods Enzymol.* **427** (2007) 139. [https://doi.org/10.1016/S0076-6879\(07\)27008-9](https://doi.org/10.1016/S0076-6879(07)27008-9)

23 M. Douglas, B. E. Bernacki, J. L. Erchinger, E. C. Finn, E. S. Fuller, E. W. Hoppe, M. E. Keillor, S. M. Morley, C. A. Mullen, J. L. Orrell, M. E. Panisko, G. A. Warren, and M. E. Wright: *J. Radioanal. Nucl. Chem.* **307** (2016) 2495. <https://doi.org/10.1007/s10967-015-4512-8>

24 A. Mally, and W. Dekant: *Food Addit. Contam.* **22** (2005) 65. <https://doi.org/10.1080/02652030500317544>

25 J. M. Brown, M. S. Boysen, S. S. Jensen, R. F. Morrison, J. Storkson, R. Lea-Currie, M. Pariza, S. Mandrup, and M. K. McIntosh: *J. Lipid Res.* **44** (2003) 1287. <https://doi.org/10.1194/jlr.M300001JLR200>

26 F. Suekane for the KamLAND collaboration: *Prog. Part. Nucl. Phys.* **57** (2006) 106. <https://doi.org/10.1016/j.pnnp.2005.12.008>

27 M. J. Anagnostakis: *Radiat. Phys. Chem.* **116** (2015) 3. <https://doi.org/10.1016/j.radphyschem.2015.04.021>

28 G. Steinhauser: *Environ. Sci. Technol.* **48** (2014) 4649. <https://doi.org/10.1021/es405654c>

29 K. Sobiech-Matura, B. Máté, and T. Altzitzoglou: *Food Control* **72** (2017) 225. <https://doi.org/10.1016/j.foodcont.2016.04.043>

30 P. P. Povinec, J. J. La Rosa, S. H. Lee, S. Mulsow, I. Osvath, and E. Wyse: *J. Radioanal. Nucl. Chem.* **248** (2001) 713. <https://doi.org/10.1023/A:1010696813200>

31 V. Cerdá: *TrAC, Trends Anal. Chem.* **118** (2019) 352. <https://doi.org/10.1016/j.trac.2019.06.001>

32 S. Arai, M. Koshimizu, Y. Fujimoto, T. Yanagida, and K. Asai: *Nucl. Instrum. Methods Phys. Res., Sect. A* **954** (2020) 161632. <https://doi.org/10.1016/j.nima.2018.11.091>

33 J. Y. Choi, K. K. Joo, H. G. Lee, and S. Y. Kim: *Curr. Appl. Phys.* **59** (2024) 182. <https://doi.org/10.1016/j.cap.2023.10.020>

34 J. K. Ahn, A. Antonelli, G. Anzivino, E. Augustine, L. Bandiera, J. Bian, F. Brizioli, S. D. Capua, G. Carini, V. Chobanova, G. D'Ambrosio, J. B. Dainton, B. Döbrich, J. Fry, A. Gianoli, A. Glazov, M. Gonzalez, M. Gorbahn, E. Goudzovski, M. Homma, Y. B. Hsiung, T. Husek, D. Hutchcroft, A. Iyer, R. W. L. Jones, M. Katayama, Y. Kawata, E. Kim, C. Kim, T. Komatsubara, K. Kotera, M. Kreps, G. Lamanna, C. Lazzeroni, S. Lezki, G. Lim, S. Lim, C. Lin, F. Mahmoudi, V. Martin, K. Massri, T. Matsumura, L. Montaldo, M. Moulson, H. Nanjo, M. Needham, S. Neshatpour, T. Nomura, D. Ogawa, K. Ono, M. Pepe, L. Peruzzo, J. Pinzino, D. Protopopescu, C. Prouve, T. Reddel, J. Redeker, D. Rinaldi, M. Romagnoni, A. Romano, A. Rostomyan, J. Sanders, D. M. Santos, I. Sarra, A. Shaikhiev, K. Shiomi, R. Shiraishi, M. Soldani, M. Sozzi, B. Stillwell, Y. Su, J. Swallow, Y. Tajima, A. Tomczak, Y. Tung, Y. Wah, R. Wanke, H. Watanabe, J. Wendel, T. Wu, M. Wynd, and G. Yang: arXiv:2501.14827 (2025). <https://doi.org/10.48550/arXiv.2501.14827>

35 Y. Shinjo, T. Kin, and A. Nohtomi: *Houshasen* **46** (2020) 39 (in Japanese). [https://doi.org/10.11470/houshasen.46.1\\_39](https://doi.org/10.11470/houshasen.46.1_39)

36 T. Yanagida and M. Koshimizu: *Phosphors for Radiation Detectors* (John Wiley & Sons, New York, 2022) pp. 39–61. <https://doi.org/10.1002/9781119583363>

37 A. Lim, A. Mahl, J. Latta, H. A. Yemam, U. Greife, and A. Sellinger: *J. Appl. Polym. Sci.* **136** (2019) 47381. <https://doi.org/10.1002/app.47381>

38 N. Hayashi and M. Koshimizu: *J. Lumin.* **277** (2025) 120993. <https://doi.org/10.1016/j.jlumin.2024.120993>

39 N. Hayashi and M. Koshimizu: *Jpn. J. Appl. Phys.* **64** (2025) 10SP06. <https://doi.org/10.35848/1347-4065/ae07ef>

40 A. Taranco'n, H. Bagán, and J. F. García: *J. Radioanal. Nucl. Chem.* **314** (2017) 555. <https://doi.org/10.1007/s10967-017-5494-5>

41 Acrylate (in Japanese): <https://www.toagosei.co.jp/products/polymer/resin/aronix.html> (accessed October 2025).